Nanoformulated Cannabidiol Attenuates Osteoarthritis-Induced Inflammation in Rat

Ravichandran Jayasuriya[1], Rajappan Chandra Sathish Kumar[2], and Ramkumar Kunka Mohanram[1],*

[1]Department of Biotechnology, School of Bioengineering, SRM Institute of Science and Technology, Kattankulathur 603 203, Tamil Nadu, India.

[2]Interdisciplinary Institute of Indian System and Medicine (IIISM), SRM Institute of Science and Technology, Kattankulathur 603 203, Tamil Nadu, India.

*Corresponding author:

Dr. K.M. Ramkumar

Professor (Research)

Department of Biotechnology, School of Bioengineering,

SRM Institute of Science and Technology, Kattankulathur 603 203, Tamil Nadu, India

Abstract

Osteoarthritis (OA) is a chronic degenerative joint disease characterized by cartilage degradation, synovial inflammation, and persistent pain. Cannabidiol (CBD), a non-psychoactive component of *Cannabis sativa*, has gained attention for its potential anti-inflammatory and analgesic properties. However, its poor bioavailability limits clinical efficacy. This study evaluates the therapeutic potential of a proprietary CBD nanoformulation in a monosodium iodoacetate (MIA)-induced rat model of knee osteoarthritis. OA was induced in Sprague-Dawley (SD) rats via intra-articular injection of MIA. And the OA rats were administered orally with CBD nanoformulation for 30 days. X-ray imaging showed a complete collapse of the femoral-tibia joint space, which was recovered by CDB nanoformulation. Histopathological analysis showed preservation of cartilage structure. Furthermore, the formulation attenuated levels of TNF-α, IL-1β, and apoptotic markers in the joint tissues, suggesting both anti-inflammatory and antioxidant effects. To check the mechanistic effect, we treated CBD nanoformulation to macrophages that were exposed to inflammatory stimulus. With modulation of oxidative stress, inflammation and ROS, CBD effectively improved the macrophage condition exposed to inflammatory stimulus. Altogether, these findings highlights the therapeutic promise of CBD nanoformulation in OA management.

Keywords: Osteoarthritis, inflammation, CBD nanoformulation, MIA-induced OA rats, macrophages

1. Introduction

Osteoarthritis (OA) is one of the major degenerative disorders that affects nearly 528 million people globally, including 23% of individuals aged more than 40 [1]. The progression of OA is characterized by progressive cartilage deterioration, synovial inflammation, and subchondral bone remodelling. This initially affects the weight-bearing capacity in joints, leading to chronic pain, stiffness, and reduced mobility of the knees [2]. The global burden of OA remains up, and in particular among patients with any metabolic disorder or commonly associated with ageing. Genetic inclinations, excessive mechanical stress, and chronic inflammatory conditions trigger the pathogenesis and progression of OA. This disorder with multifactorial etiology remains a challenge due to the progressive nature of cartilage degeneration, the limited regenerative capacity of chondrocytes, and the incomplete efficacy of current treatment options [3].

At a cellular perspective, the chondrocytes, which are the resident cells of articular cartilage, play a key role in maintaining homeostasis, achieved by a balanced synthesis and degradation. This programmed function is lost due to elevated inflammatory signals in the case of OA [4]. As the disease progresses, the pro-inflammatory signaling, such as TNF-α, IL-1β, and IL-6 secreted by synovial fibroblasts and macrophages, drives chondrocyte apoptosis, oxidative stress, and extracellular matrix (ECM) breakdown. Oxidative stress-induced accumulation of intracellular reactive oxygen species accelerates senescence in chondrocytes. The increase in cytokines like TNF-α and IL-1β activates caspase-dependent apoptosis, ultimately triggering chondrocyte death [5].

Anti-inflammatory agents like corticosteroids or non-steroidal anti-inflammatory drugs (NSAIDs) are potent in reducing inflammation, and are administered to patients with inflammatory syndromes, including OA [6]. Though they are associated with symptomatic

relief, they fail to halt disease progression. Moreover, long-term administration of these agents is associated with cardiovascular and gastrointestinal risks [7]. Corticosteroids, while they can relieve inflammation, are not antioxidants themselves, which are essential to overcome cellular stress observed in OA [8]. Given these limitations, the quest for safer yet disease-controlling alternatives has begun to intensify. On the other hand, one promising area of research is the endocannabinoid system that serves as a key regulator of inflammation, pain perception, and cartilage homeostasis.

The endocannabinoid system plays a vital role in maintaining joint integrity by modulating nociceptive signaling, immune responses, and chondrocyte metabolism. While this system plays an important role in joint homeostasis and pain modulation, its dysfunction has been implicated in the progression of OA [9]. Beyond this endocannabinoid system, oxidative stress-triggered antioxidant deficit is crucial in the pathogenesis of OA. Altogether, this leads to excessive inflammation, chondrocyte apoptosis, and cartilage degradation [10]. To address these pathological hallmarks, agents that exhibit anti-inflammatory and anti-apoptotic properties, yet with fewer proven side effects, need exploration.

Cannabidiol (CBD), a non-psychoactive phytocannabinoid derived from *Cannabis sativa*, has gained interest as a potential therapeutic agent for chronic inflammatory conditions. CBD is known to interact with a bunch of key molecular targets that are involved in inflammation, oxidative stress, and cellular survival, making it a promising candidate for OA therapy [11]. Moreover, preclinical studies have shown the protective effect of CBD in significantly decreasing the key inflammatory markers like TNF-α, IL-1β, and IL-6, which are central to the pathogenesis of OA [12, 13]. Excessive synthesis and activation of MMPs, in particular MMP-13, trigger OA pathogenesis, as they are involved in the degradation of type II collagen, a major component of cartilage. In line with this, CBD helps recover cartilage degradation by limiting the activity of MMP-13 and thus promoting collagen deposition in

the articular chondrocytes [14]. Beyond this, CBD also has analgesic properties that help perception of joint pain, possibly by integrating with transient receptor potential vanilloid 1 (TRPV1) channels that are involved in nociception [15, 16].

Having these advances, the protective effect of CBD extracts has been extensively studied [17, 18], which critically lacks the clinical relevance due to the use of non-pharmaceutical grades, and potential variability in delivery system, bioavailability, and dosing regimens. To bridge this gap, we in this study are evaluating a standardized, nano-enhanced CBD formulation in a monosodium iodoacetate (MIA)-induced osteoarthritis rat model. Unlike previous studies that used crude extracts, we focused on the optimized formulation and delivery relevant to clinical settings. While detailed pharmacokinetic or tissue distribution analyses were beyond the scope of this study, the use of a formulation designed for clinical application adds value by mimicking realistic treatment conditions.

2. Materials and methods

2.1. Preparation and characterization of CBD nanoformulation

The Cannabidiol (CBD) nanoformulation was provided by Unique Therapeutics Global, Czech Republic. The formulation was developed using their proprietary emulsification method. As the formulation is proprietary, exact composition and methods are not disclosed.

The particle size and zeta potential of the CBD nanoformulation were characterized using a Zetasizer Nano ZS (Malvern Panalytical, UK). Dynamic light scattering (DLS) was used to determine the hydrodynamic size, and laser Doppler electrophoresis was used for zeta potential analysis. All measurements were conducted at 25 ± 0.1 °C in deionized water. For measurement of zeta potential, the sample was loaded into clear disposable zeta cell with an attenuator setting of 7, and 12 runs/sample were performed. Particle size was assessed using disposable sizing cuvettes with an attenuator setting of 6, and a 60 s measurement window.

The size and zeta potential data were processed using the instrument's standard software (Zetasizer v8.01.490).

2.2. Animal maintenance

The male Sprague Dawley (SD) rats were procured from Mass Biotech, Chengalpattu, and housed in IVC cages at the specific pathogen-free (SPF) animal facility at SRMIST, Chennai, at a rate of 2 animals per cage. The procured animals were quarantined for 10 days before the start of the experiment. The animals were given free access to a standard pellet diet and water ad libitum, and were adapted to a 12 h cycle of light and dark at a room temperature of 22–24 °C, during the quarantine period, and continued till the end of the experiment. All experimental procedures were approved by an Institutional Animal Ethical Committee (SAF/IAEC/240502/003).

2.3. Dose fixation studies

An acute toxicity study was performed to evaluate the safety profile of CBD nanoformulation on SD rats. Rats weighing 100-120g were randomly divided and administered with CDB nanoformulation at doses, 50, 100, 150, and 200 mg/kg-b.w. intragastrically using an oral gavage, for a continuous 14 days. Each group carried 2 animals randomly, and the control group (2 animals) was not administered with CBD or any other drug for 14 days. During this period, no animals were restricted from any of their routine activities, including consumption of food and water. No analgesics or anaesthetics were administered to the experimental rats during this period. Care was taken to dose each animal at a 24-hour interval for a continuous 14 days. The doses selected in this study were based on a previous literature [20], where hemp-derived CBD isolate administered to SD rats showed no adverse effect up to 150 mg/kg-b.w./day.

The animals were visually examined for any illness or mortality symptoms every day, immediately after administration of the drug, for all 14 days. Animal weight was monitored every 3 days, and the dosage was calculated accordingly. All animals were fasted overnight on the 14th day, and were euthanized on the 15th day by intraperitoneal injection of ketamine (150 mg/kg b.w.) and xylazine (20 mg/kg b.w.). Blood was withdrawn from the tail vein to monitor fasting blood glucose using a digital glucometer. Immediately after euthanasia, blood samples were collected in a non-heparinised tube through cardiac puncture, serum was isolated and processed for biochemical analysis. The vital organs, such as the liver, kidney, pancreas, heart, and spleen, were carefully extracted from the animal, washed, and stored in 10% neutral buffered formalin for histopathological analysis.

2.4. Estimation of biochemical parameters

The biochemical parameters, including liver function tests (ALT, AST, ALP, Bilirubin, Total Protein), renal function markers (BUN, Creatinine), and serum electrolytes, were analyzed using an autoanalyzer calibrated with rat-specific standards.

2.5. Induction of knee osteoarthritis

To demonstrate the model of OA in rats, we used monosodium iodoacetate (MIA), which induces cartilage degeneration as seen in humans with OA. The animals were anesthetised by intraperitoneal injection of ketamine (70 mg/kg b.w.) and xylazine (5 mg/kg b.w.). After anaesthesia, the animals were immediately transferred to a heating pad, set at 37 °C. Lubricant eye drops were administered to both eyes of the animals after anaesthesia, to prevent corneal irritation during recovery. Hair removal was performed using a trimmer in both the knee region, and to note, no hair removal cream was used. The knee site was sterilised using 70% ethanol and 5% povidone-iodine solution i.p. before injection to maintain an aseptic environment. 3 mg of MIA, dissolved in sterile normal saline, 50 µL was

delivered to the knee site directly through an intraarticular puncture [21, 22]. The knee was held upright at 90 degrees, needle was inserted through the patellar tendon. Care was taken not to mechanically disturb the articular cartilage or meniscus using the needle during intraarticular injection. Immediately after delivery of MIA, the needle is withdrawn, and the area was again sterilised with 70% ethanol and 5% povidone-iodine solution i.p. The animals were caged back after complete recovery of anaesthesia, and were observed for any signs of illness. The animals were not restricted to any of their routine activities till the end of the experimental procedure.

2.6. Administration of CBD nanoformulation

MIA-mediated cartilage damage typically starts after 7 days, and hence, to have a moderate to severe damage of cartilage membrane, we started dosing the rats after 14 days from the day of MIA-injection. We ensured that the animals were able to move freely in the cage and had no injuries on the external surface (or the surface of the skin) of the knee before the start of treatment. As per our acute toxicity data, we did not notice any significant damage in the vital organs or in the biochemical parameters estimated when exposed to CBD nanoformulation up to a concentration of 200 mg/kg/day for a continuous 14 days (detailed in the results section). Hence, in the efficacy study, we fixed two concentrations, such as 100 and 200 mg/kg body weight per day, representing a low dose and a high dose.

The experimental groups included control animals with no OA or CBD exposure (n=8), the rats that were injected with MIA in both knees stands the OA group (n=8), the OA rats administered with 100 mg/kg CBD nanoformulation daily representing a low dose exposure (n=10), and a 200 mg/kg group, representing high dose exposure (n=10). The animals were fed with standard chow diet, and no changes were made to the standard feed and water. Neither the MIA-injected nor the control animals were given any anti-inflammatory

drugs/agents throughout the study period. The obtained CBD formulation was in a liquid consistency, and no further diluents or vehicles were used. The CBD formulation was administered to rats at the desired concentration in low and high dose groups using an oral gavage, and we ensured a 24-hour interval between every dose.

2.7. Radiological assessment of knee osteoarthritis

The rats, after 30 days of MIA injection, were examined for any changes in femoro-tibial joint space by X-ray radiograph. The rats were anesthetised by intraperitoneal injection of ketamine (80 mg/kg b.w.) and xylazine (5 mg/kg b.w.), administered with eye drops, and their knees were radiographed at 40 KV and 0.5 mA/s. After generating radiographs, the animals were recovered, and the following day, the animals were euthanized as mentioned earlier, and the knee samples were extracted, stored in 10% neutral buffered formalin for histopathological analysis.

2.8. Cell culture and treatment

To study the action of CBD nanoformulation on inflammatory parameters, we used IC21 macrophages in this study. The IC21 macrophages were cultured in RPMI 1640 medium (Sigma, USA) with 10 % fetal bovine serum (FBS, Gibco, USA) on a humidified incubator with 5% CO2. The stock CBD nanoformulation obtained from Unique Therapeutics was at a concentration of 600mg/30mL (i.e., 20 mg/mL). Since the formulation is water soluble, further dilutions were made in nuclease-free water (Qiagen, USA) and supplemented to the cells along with culture medium at appropriate concentrations. The stock as well as the sub-stock were stored at 4 °C as recommended by the manufacturer. To induce inflammation, the IC21 macrophages were induced with LPS (Santa Cruz, USA) and IL-1β (Invitrogen, USA) at a concentration of 1 μg and 10 ng per mL, respectively, adapted from Calabrese et al. [19]. This cocktail is henceforth referred to as an inflammatory stimulus (IS). The IC21

cells were treated with CBD nanoformulation at the desired concentration by directly adding an appropriate volume to the culture medium before being induced with IS.

2.9. Cellular viability assay

The IC21 macrophages were seeded on a 96-well culture plate overnight with low serum (1% FBS) medium. After this, the cells were incubated with varying concentrations of CBD nanoformulation for 24 hours. The cells were incubated with 0.1% Alamar blue solution (Bio-Rad, USA) for about 4 hours. Then, the absorbance was recorded at a wavelength of 570 and 600 nm. The viability of cells upon exposure to CBD nanoformulation was then evaluated using an untreated control.

2.10. Assay for measurement of NO production

NO production was assayed by measuring the nitrite concentration in the supernatant of cultured IC21 macrophages with or without CBD formulation under IS. The cells were seeded in a 96-well culture plate and treated with CBD formulation before inducing IS. About 100 µL of supernatant was recovered after the treatment and transferred to a sterile 1.5 mL Eppendorf tube. The content is then centrifuged at 10,000 rpm to remove any floating cells that could interfere with the assay. The clear supernatant is then transferred to a new 96-well culture plate and mixed with an equal volume of Griess reagent (1% sulphanilamide, 0.1% naphthyl ethylenediamine dihydrochloride, and 2.5% H_3PO_4). This content was then incubated in the dark for 10 minutes, followed by measurement of nitrite concentration by measuring the absorbance at 570 nm.

2.11. RNA isolation and qPCR

After the treatment period, the rats were euthanized, and knee joints covering cartilage, synovium, and subchondral bone tissues were cut, snap-frozen, and stored at –80°C until RNA isolation. About 100 mg of frozen knee sample was taken and ground using liquid

nitrogen in a pre-chilled mortar and pestle. The environment was maintained RNase-free by cleaning the surface with RNase destroyer. RNaseOUT Recombinant Ribonuclease Inhibitor (Invitrogen) was added to the sample to inhibit the activity of RNases in the knee sample. About 500 µL TRIzol RNA isolation reagent (Takara, Japan) was added to the ground tissues and mixed thoroughly, and incubated on ice. Following this, about 250 µL of chloroform was added to the homogenate and pipette-mixed, and stored on ice. Similarly, the cultured macrophages after experimental conditions were harvested and immediately lysed with 250 µL TRIzol reagent for about 30 min, followed by incubation in about 100 µL of chloroform for an additional 10 min, and maintained on ice. The homogenates obtained from rat knees as well as from the cultured cells were centrifuged to get a clear RNA-containing supernatant, which was transferred to a clean tube. This supernatant was then mixed with an equal volume of 70% ethanol, and the contents were transferred to a spin column included in the RNeasy kit (Qiagen, USA), and RNA isolation was performed following the manufacturer's instructions. The final eluent was stored and reverse transcribed to cDNA using ABScript II cDNA first-strand synthesis kit (ABclonal, Canada). Gene expression analysis for targets was determined using SYBR green fast qPCR mix (ABclonal, Canada) on a CFX connect real-time PCR (Bio-Rad, USA). GAPDH served as an internal control.

2.12. Protein extraction and western blotting

Whole cell protein extraction from rat knees was performed using RIPA buffer. In brief, the snap-frozen knee samples were ground by adding an adequate volume of RIPA buffer. The homogenate was then maintained on ice, and further lysed by a brief 5 sec vortexing for an hour at every 10 min interval. The homogenate was then centrifuged at 12,500 rpm to get a clear supernatant. The protein concentration was quantified by Bradford's assay reagent. About 40 µg of total protein was electrophoresed on an SDS gel and transferred to a nitrocellulose membrane. The membrane was then blocked and incubated with the primary

antibody overnight at 4 °C. Following this, the membrane was washed and incubated with a secondary antibody. The blots were then imaged using an ECL kit on a chemidoc to check the target protein expression. β-actin serves as an internal control.

2.13. Statistical analysis

The data given in this manuscript are represented as mean ± standard deviation. One-way ANOVA was performed to determine the statistical significance. The experiment is considered significant only if $p<0.05$. All analysis and bar graphs were plotted on a GraphPad Prism software (v. 8.01).

3. Results

3.1. Characterization of CBD nanoformulation

As represented in the Figure S1a, the zeta potential of the formulation was observed as to be -6.11 mV, confirming the surface charge distribution and colloidal stability of the nanoemulsion. The negative charge of the formulation promises enhanced colloidal stability and reduced aggregation, because of which the drug exhibits lower toxicity and longer circulation, when delivered systemically. The particle size and zeta potential of the CBD nanoformulation was analyzed and showed that 95.2% of particles measured approximately 14.26 d.nm in diameter (Z-average: 91.42 d.nm), indicating a predominantly monodisperse formulation (Figure S1b).

3.2. Acute toxicity assessment of CBD nanoformulation exposed to SD rats

Following the administration of doses calculated based on body weight, no signs of mortality or illness were observed in any of the rats during the 14-day study period. As shown in Figure S2a, all groups exhibited a consistent increase in body weight, with measurements recorded every 3 days. Furthermore, no significant differences in food intake (Figure S2b) or fluid

consumption (Figure S2c) were observed between the control and CBD-administered groups. Both food and water intake gradually increased in correlation with the animals' weight gain, with average water consumption ranging from 10 to 20 mL every 3 days. These results suggest that the drug did not negatively impact the overall health or growth of the animals, nor did it disrupt normal feeding or hydration patterns.

Additionally, the weights of key organs such as the liver and kidneys, which are critical for metabolism and excretion, were measured. No significant changes in organ weights were detected between the groups, with both liver and kidney weights (organ to body ratio) remaining within normal ranges (Figure S2d). This indicates that the CBD nanoformulation did not adversely affect the structure or function of these vital organs. Blood glucose levels were measured on the 15^{th} day following a 12-hour fasting period. No significant differences in blood glucose were found across the experimental groups, with levels ranging between 95 and 115 mg/dL (Figure S2e), indicating that the CBD nanoformulation did not affect glucose regulation in the rats.

The liver function markers such as AST, ALT, and ALP levels were measured in the serum of the experimental groups, as shown in the Figure S3. AST (Figure S3a) and ALT (Figure S3b) levels ranged between 100 and 130 IU/L, with no significant differences observed between the groups. Similarly, ALP (Figure S3c) levels ranged from 200 to 210 IU/L, showing no significant variation across the treatment groups. Additionally, bilirubin (Figure S3d) and total protein (Figure S3e) levels were estimated to be approximately 0.5 mg/dL and 6 mg/dL, respectively, with no significant differences among the experimental groups.

To evaluate kidney function, blood urea nitrogen (BUN) and creatinine levels were measured in the serum of the experimental rats. As shown in the Figure S3f, BUN levels ranged from approximately 15 to 18 mg/dL, with no significant changes observed in the groups treated

with the CBD nanoformulation. Similarly, creatinine levels were measured between 0.3 and 0.4 mg/dL, again showing no significant differences among the experimental groups (Figure S3g).

We assessed the lipid profile in the serum of experimental rats by measuring the levels of cholesterol, high-density lipoprotein (HDL), low-density lipoprotein (LDL), and triglycerides (TGL). The results indicated that cholesterol levels ranged between 40-60 mg/dL (Figure S3h), HDL levels ranged from 30-35 mg/dL (Figure S3i), LDL levels were between 25-30 mg/dL (Figure S3j), and TGL measured between 180-200 mg/dL (Figure S3k). Notably, no significant differences were observed across the experimental groups, indicating that the CBD nanoformulation did not adversely affect lipid metabolism or overall cardiovascular health. In addition, the key electrolytes in the serum of experimental rats, including sodium, potassium, and chloride, were also found to have no significant difference between control and the highest dose administered, i.e., 200 mg/kg.

3.2. Histological assessment of vital organs in SD rats exposed to CBD nanoformulation

In addition to the biochemical parameters, we assessed histopathological changes in both control rats and those exposed to a high dose of 200 mg/kg body weight of the CBD nanoformulation. As illustrated in Figures S3a-b, there were no signs of hepatotoxicity in either the control or the 200 mg/kg group, with healthy hepatocytes and normal sinusoids indicated by the black and yellow arrows, respectively. Figures S3c-d depict the kidneys, showing healthy structures with the black arrow highlighting the healthy glomerulus in both the control and high-dose groups. Furthermore, Figures S3e-f illustrate the pancreas, demonstrating the integrity of the β-cell architecture (represented by black arrows) in both the control and 200 mg/kg groups. Figure S4g-h represents normal myocardium (black arrow heads) with no marked inflammation, and normal-shaped nuclei (yellow arrow head) in

control or the 200 mg/kg group. Figure S4i-j represent the spleen with normal architecture of the red pulp (yellow arrow heads) and the white pulp (black arrow heads) in both control and CBD-exposed groups. These histopathological findings collectively reinforce the conclusion that the CBD nanoformulation does not induce toxic effects on the liver, kidneys, or pancreas, suggesting that the treatment is safe and well-tolerated at the administered dosage.

3.3. Effect of CBD nanoformulation on the knees of OA rats

OA is associated with gait alterations, and hence, we first evaluated the effect of CBD nanoformulation on these impairments. Compared to control rats, the stride length was significantly reduced in OA rats. This decrease possibly reflects joint stiffness, inflammation, and pain that would cause abnormalities in the gait pattern. However, treatment with CBD nanoformulation improved stride length in a dose-dependent manner. The high-dose group (200 mg/kg) exhibited a greater restoration of stride length compared to the low-dose group (100 mg/kg), indicating its potential in alleviating OA-associated gait impairments and enhancing joint function (Figure 1a).

Radiological evaluation through X-ray imaging is a fundamental approach to assessing structural changes in OA. In the control group, the bicondylar joint appears normal, with well-preserved joint space, smooth bone surfaces, and no signs of abnormal mineralization, reflecting healthy cartilage and bone integrity. However, in the OA group, significant structural damage is observed, as represented in Figure 1b. The loss of cartilage leads to direct bone-on-bone contact, causing bone resorption and sclerosis, a condition where the bone becomes abnormally dense due to increased mechanical stress and inflammatory responses (marked as I in Figure 1b). Severe sclerosis and inflammatory changes further contribute to bone deformities, compromising joint function and mobility. The CBD-treated groups (low dose and high dose) exhibit notable improvements in bone structure. While some

signs of sclerosis and deformity persist, there is a visible reduction in bone mineral density abnormalities, suggesting a protective effect of CBD against excessive bone remodelling. The high-dose CBD group shows better joint preservation compared to the low-dose group, indicating a dose-dependent therapeutic effect. These findings highlight the potential of CBD nanoformulation in mitigating OA-associated bone degeneration by reducing sclerosis, preserving joint space, and minimizing structural deformities, ultimately aiding in joint recovery.

We furthered to Kellgren-Lawrence (K-L) scoring to assess OA severity based on the radiographs. The control group exhibited no features of OA, with a well-defined gap between the tibia and femur, and was thus classified as Grade 0. In contrast, the OA group displayed severe joint space narrowing, pronounced sclerosis, and bone deformities, corresponding to Grade 4. The CBD low-dose (100 mg/kg) group exhibited moderate osteophyte formation, though not as severe as the OA group. Additionally, some degree of sclerosis and possible bone deformities were observed, making them categorised under Grade 3. Although the joint space was not completely restored to that of the control group, OA animals treated with a high dose of CBD (200 mg/kg) showed improved joint space preservation with only mild sclerosis, scoring Grade 2. Overall, OA rats were initially classified as Grade 4, but CBD treatment dose-dependently improved joint condition, reducing the severity to Grade 2 at the 200 mg/kg concentration.

The diameter of the knee joint was measured using a digital vernier caliper. As shown in Figure 1c, the OA group displayed a significant increase in joint diameter compared to the control group, indicative of pronounced periarticular edema and synovial inflammation associated with OA progression. In contrast, treatment with the CBD nanoformulation resulted in a dose-dependent reduction in knee diameter, with both low- and high-dose groups exhibiting a statistically significant decrease, suggesting attenuation of inflammation and

joint swelling. Gross morphological assessment revealed that control animals had smooth, congruent articular surfaces at both the tibial plateau and femoral condyles, with no visible signs of cartilage erosion or joint deformation. However, OA-induced knees exhibited marked surface irregularities, cartilage thinning, and swelling, with exposed subchondral bone particularly evident in the medial tibial plateau and femoral groove. Additionally, osteophyte-like bony projections were noted in the peripatellar and intercondylar regions, consistent with severe joint remodelling. In the CBD low-dose group, the joint surface showed partial preservation, with reduced surface roughness and limited exposure of subchondral bone. The high-dose CBD group demonstrated a more intact articular morphology, with relatively smooth joint surfaces and minimal osteophytic outgrowth, closely resembling the control group. However, these changes in detail are evaluated through histological analysis, detailed in the forthcoming sections.

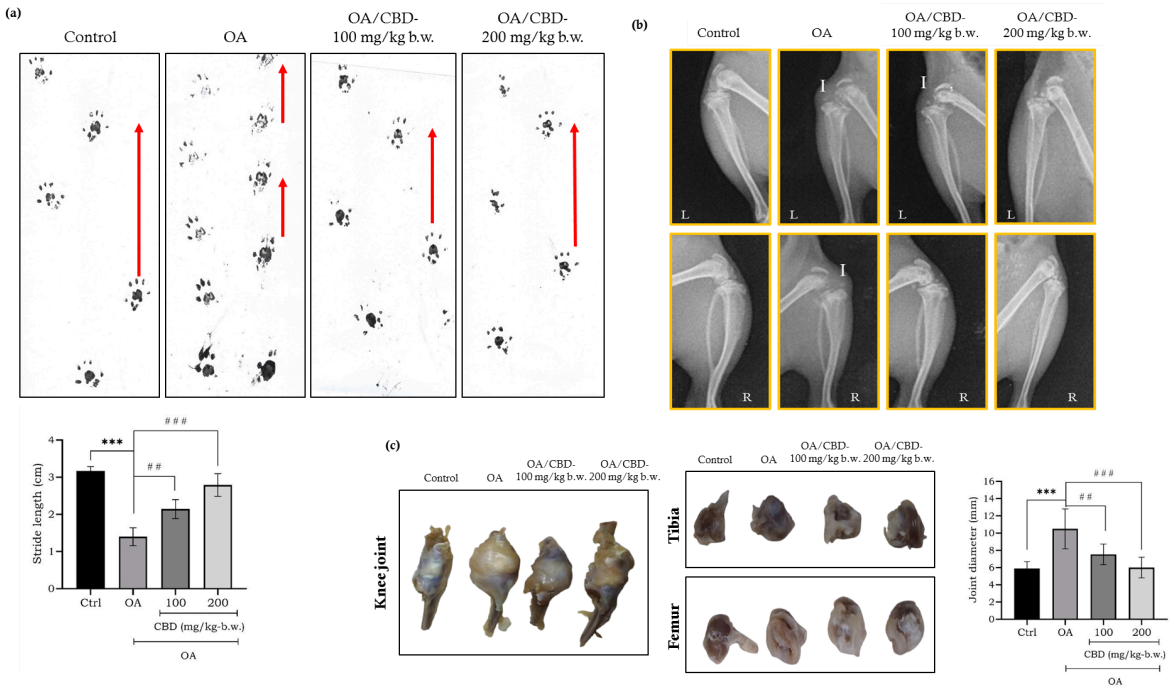

Figure 1: Stride length measurement (a) in OA rats treated with CBD nanoformulation. Radiological assessment (b) and measurement of joint diameter (c) among the experimental

groups. Data in the bar graph are represented as mean ± S.D. *p<0.05, **p<0.01, ***p<0.001. *compared to control; #compared to OA.

3.4. Effect of CBD nanoformulation on the cartilage degradation in OA rats

The histological evaluation of knee joint sections revealed distinct differences in cartilage integrity across the experimental groups, depicted in the Figure 2a (i-iv). The control group (i) exhibited smooth and well-preserved articular cartilage, with a clearly defined structure and intact surface. The joint space appeared uniform, indicating the absence of degenerative changes (pointed with red arrowhead). Whereas the knees of the OA group were observed with severe degradation of cartilage (ii). A complete collapse of the cartilage region was observed, with severe loss of structural integrity and the absence of a distinct cartilage layer. The joint surface appeared highly irregular, and the intra-articular space was significantly reduced, reflecting the advanced degenerative changes characteristic of osteoarthritis. However, the sections from CBD nanoformulation-treated groups showed a dose-dependent variation in cartilage preservation. The low-dose group (100 mg/kg b.w.) displayed notable cartilage deterioration similar to the OA group, with a lack of distinct layering and significant surface disruption (iii). And, the high-dose group (200 mg/kg b.w.) exhibited mild integration within the intra-articular spaces, suggesting a partial protective or reparative effect (iv). Even though CBD did not completely restore the cartilage structure, it showed a remarkable difference compared to severe degeneration as seen in the knees of the OA group.

To have a clear picture of cartilage degradation and formation, we stained the sections of experimental groups with Safranin-O dye (Figure 2b (i-iv)), which is typically used to evaluate cartilage health by detecting glycosaminoglycans and proteoglycans in the extracellular matrix. Cartilage degeneration as seen in OA is linked to loss of proteoglycans, and hence, Safranin-O could serve as a key indicator to check the integrity of articular

cartilage in the knees of experimental rats. The cartilage in the control group shows strong and uniform Safranin-O staining, indicating a high proteoglycan content and well-preserved cartilage (i). In the OA group, staining is almost absent, suggesting severe cartilage degradation and a significant loss of proteoglycans, which are essential for maintaining cartilage integrity (ii). Although uneven staining remains in the low-dose group, the cartilage remains structurally compromised compared to the control, indicating a partial restoration (iii). The staining intensity is higher and more cartilage preservation in the control group in the 200 mg/kg group, suggesting a greater retention of proteoglycans (iv).

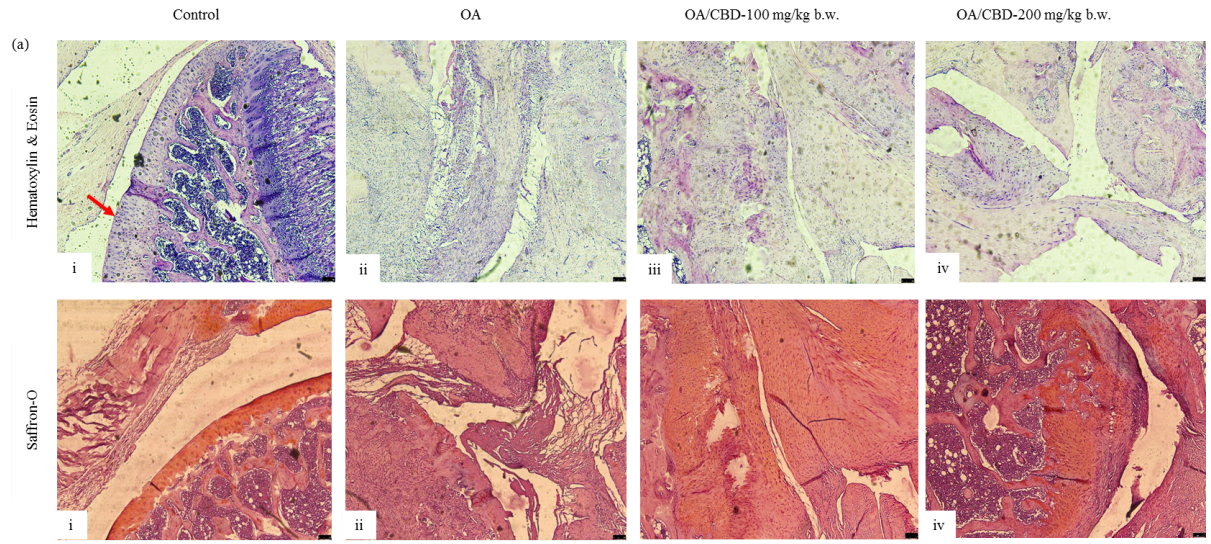

Figure 2: Histological assessment of articular cartilage (a) and cartilage staining using saffron-O (b) in control (i), OA (ii), and OA rats treated with CBD nanoformulation at 100 mg/kg-b.w. (iii), and 200 mg/kg-b.w. (iv).

3.5. Effect of CBD nanoformulation on the inflammatory parameters in OA rats

While acute inflammation is a protective mechanism aimed at clearing damaged cells and initiating tissue repair, chronic inflammation can contribute to cartilage degradation, as seen in OA (Figure 3a (i-iv)). While no infiltration of inflammatory cells is observed in the control group (i), a dense accumulation of acute inflammatory cells, likely leukocytes, is present in the OA group (ii) and the CBD low-dose group (iii). This suggests a heightened

inflammatory response, which is characteristic of cartilage degradation and OA progression. A noticeable reduction in inflammatory cell recruitment, indicating the potential anti-inflammatory effect of CBD nanoformulation, is observed in CBD high-dose treated groups (iv). This mitigation of excessive inflammatory cell infiltration would promote a more favourable condition for cartilage repair.

We furthered our notion to better understand inflammation by assessing the markers in circulation and the knee joint. As represented in the Figure 3b, the concentrations of CRP, IFN-γ, and IL-6 were significantly higher ($p<0.001$) in the serum of OA-induced rats. This increase was then decreased in a step-wise manner upon treatment with CBD nanoformulation in 100 and 200 mg/kg concentrations. Along with this, the mRNA expression of inflammatory markers in the knees of OA rats was also assessed. This also revealed that the inflammatory markers such as TNF-α and IL-1β were significantly increased in expression in the OA rats (Figure 3c). However, treatment with CBD nanoformulation reversed this by significantly inhibiting the inflammatory mediators such as TNF-α and IL-6 at 200 mg/kg concentrations ($p<0.01$).

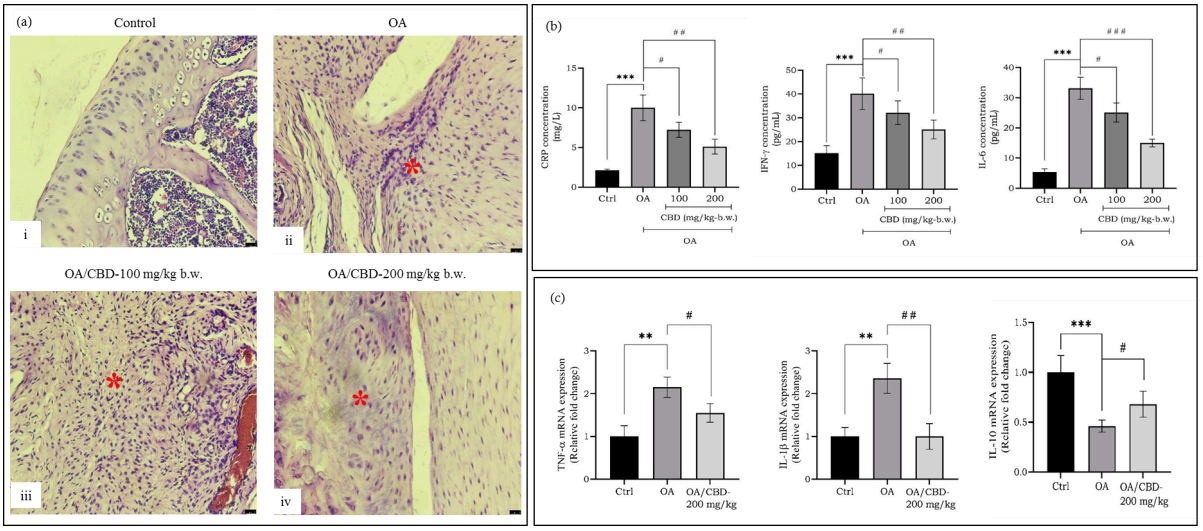

Figure 3: Histological assessment of articular cartilage showing the inflammatory status among the experimental groups (a). Assessment of serum inflammatory cytokines (b) and

mRNA expression of inflammatory makers in the knee joints (c) among the experimental groups. Data in the bar graph are represented as mean ± S.D. *p<0.05, **p<0.01, ***p<0.001. *compared to control; #compared to OA.

3.6. Effect of CBD nanoformulation on the arrangement of chondrocytes in OA rats

To have a deeper look into the cellular perspective that is involved in cartilage regeneration, we observed the histomorphology of chondrocytes between the experimental groups using H&E staining. As represented in the Figure 4a (i), the articular cartilage in the knees of control rats exhibited a well-structured arrangement of chondrocytes across the superficial (S), transitional (T), and radial (R) zones. The superficial zone contained small, flattened chondrocytes aligned parallel to the articular surface, while the transitional and radial zones displayed more rounded chondrocytes organized into columns. These chondrocytes were housed within lacunae, forming characteristic cell nests, indicative of healthy cartilage. In contrast, the knees of OA rats exhibited severe cartilage degradation with no well-organized chondrocytes observed (Figure 4a (ii)). Notably, lacunae were absent, leaving no structural compartments to house chondrocytes. The few remaining chondrocytes appeared shrunken, disorganized, and irregularly shaped (red arrowhead), suggesting extensive cartilage damage and cellular degeneration.

In the low-dose CBD (100 mg/kg) treated group ((Figure 4a (iii))), some lacunae were present, though they appeared empty (white arrowheads) or sparsely populated. The few chondrocytes observed were not well-defined, displaying irregular morphology and a lack of proper organization within the cartilage matrix. The high-dose CBD-treated group (200 mg/kg) demonstrated a more noticeable presence of chondrocytes compared to the OA and low-dose groups. However, despite this apparent recovery, the chondrocytes were not organized into the distinct three-zone structure observed in the control group (Figure 4a (iv)).

Instead, they were dispersed irregularly throughout the cartilage, suggesting partial restoration but not complete regeneration of cartilage architecture as seen in control knees.

We then studied the protein expression of apoptosis-related proteins in the knee of OA rats (Figure 4b). We found a significant decrease in the protein expression of SOD2 in the knee of OA rats, a key antioxidant enzyme responsible for controlling cellular distress. In line with the expression of SOD2, there was a tremendous increase in the Bax/Bcl2 ratio ($p<0.01$) and cleaved caspase 3 expression ($p<0.001$). Elevated levels of these proteins trigger apoptotic machinery, thereby possible loss of chondrocytes and cartilage degradation. This phenomenon is, however, reversed by CBD administration at 200 mg/kg, which increases SOD2 levels and decreases the Bax/Bcl2 ratio and cleaved caspase 3 expression.

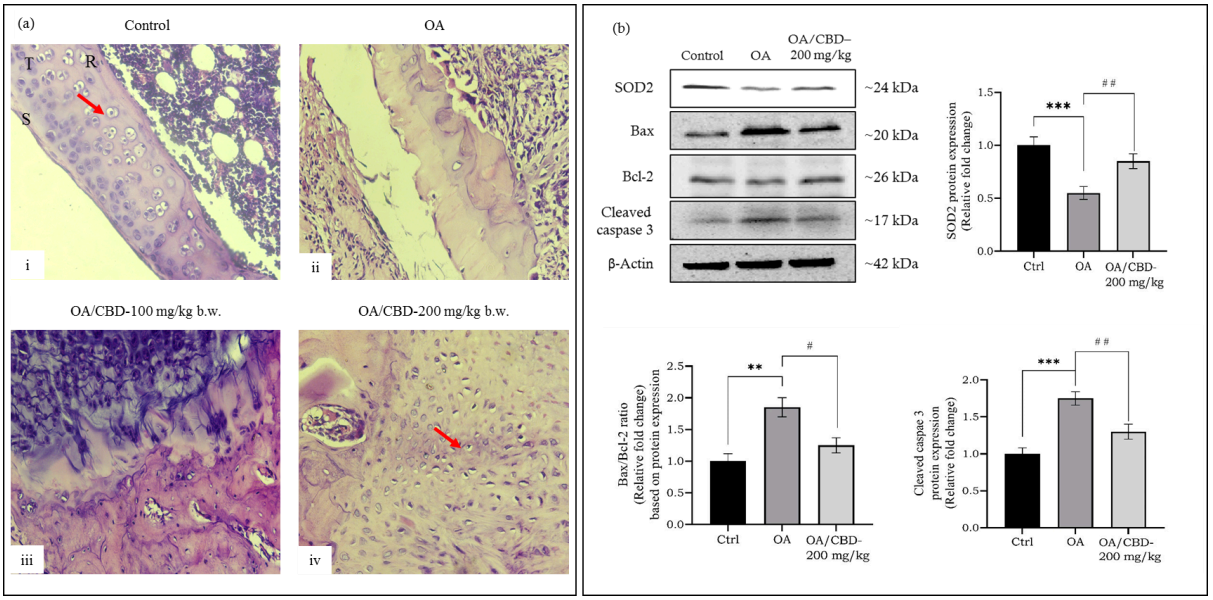

Figure 4: Histological assessment of articular cartilage showing the status of chondrocytes among the experimental groups (a). Expression of proteins such as SOD2, Bax, Bcl-2, and cleaved caspase-3 from the knee joints of experimental rats (b). Data in the bar graph are represented as mean ± S.D. *$p<0.05$, **$p<0.01$, ***$p<0.001$. *compared to control; #compared to OA.

3.7. Anti-inflammatory role of CBD nanoformulation in macrophages exposed to an inflammatory stimulus in vitro

While CBD showed its potential in reducing inflammation, we ought to perceive its role at the cellular level, hence, the macrophages, an ideal choice to study inflammation, were recruited. Firstly, the non-toxic concentration of CBD nanoformulation was determined using the Alamar blue assay. As seen in the figure, a dose-dependent decrease in the viability of IC21 macrophages, with significance $p<0.001$, was observed at more than 0.2 μg/mL of formulation. No significant cell death was observed at 0.1 μg/mL concentration, whereas less than 15% death (85% viability) was observed at 0.2 μg/mL concentration (Figure 5a). Hence, we fixed 0.1 and 0.2 μg/mL as low and high doses to study the effect of formulation for to rest of this study.

The expression of pro-inflammatory and anti-inflammatory cytokines was assessed to evaluate the anti-inflammatory potential of CBD nanoformulation. As seen in Figure 2b-e, the expression of pro-inflammatory cytokines such as TNF-α ($p<0.001$), IFNγ ($p<0.01$), IL-6 ($p<0.001$), and IL-1β ($p<0.001$) increased with a fall in the expression of IL-10 (Figure 2f) in IS-induced IC21 macrophages. It is also evident that CBD pretreated IC21 macrophages were observed with significantly decreased pro-inflammatory cytokines and increased anti-inflammatory cytokines, IL-10 in a dose-dependent manner.

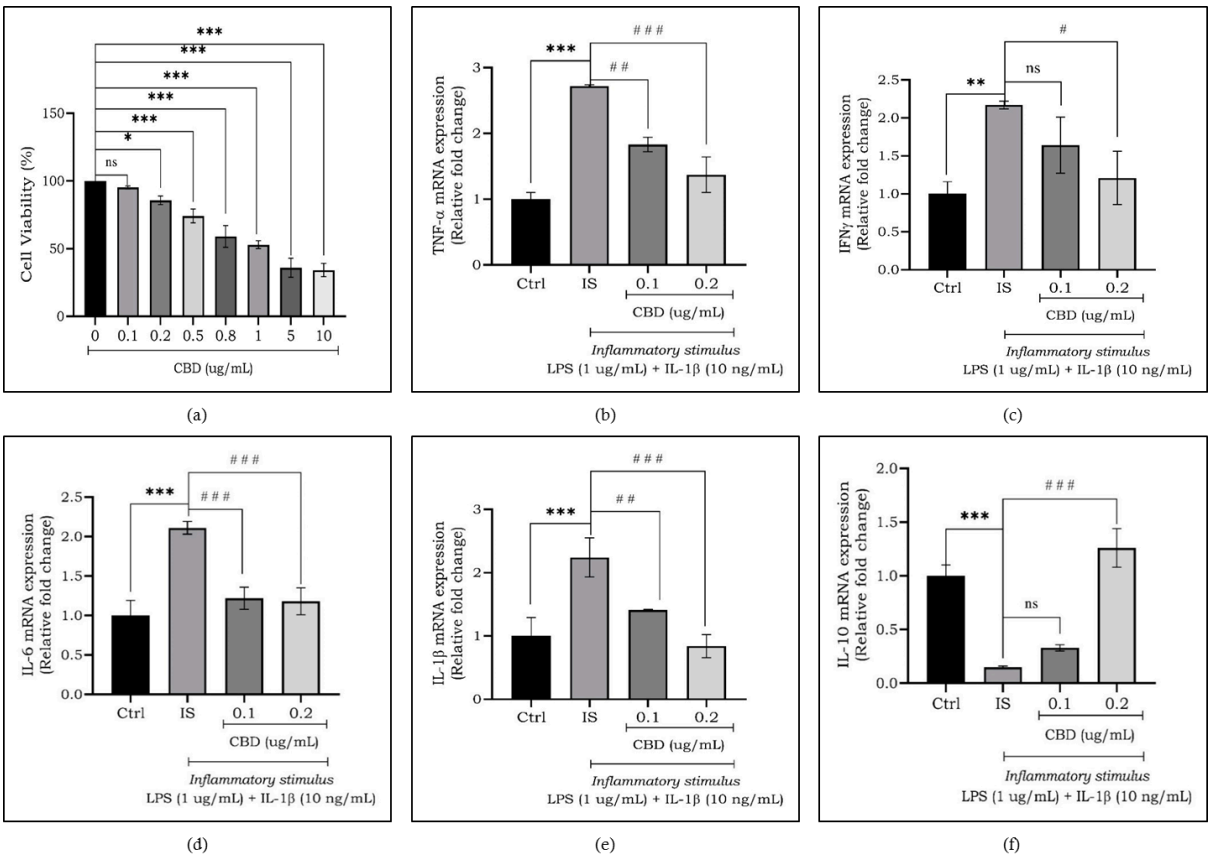

Figure 5: Viability of IC21 macrophages on exposure to different concentrations of CBD nanoformulation (a). Effect of CBD nanoformulation on the mRNA expression of inflammatory cytokines such as TNF-α (b), IFN-γ (c), IL-6 (d), IL-1β (e), and IL-10 (f) in IC21 macrophages exposed to IS. Data in the bar graph are represented as mean ± S.D. *p<0.05, **p<0.01, ***p<0.001. *compared to control; #compared to IS. IS in the figure represents inflammatory stimulus.

3.8. Effect of CBD nanoformulation on the intracellular ROS and oxidative stress in macrophages exposed to an inflammatory stimulus in vitro

Following inflammation, we studied the oxidative stress markers to elucidate the capacity of CBD to quench oxidative stress in macrophages triggered by an inflammatory stimulus. As expected, we observed an increased expression of oxidative stress markers TXNIP ($p<0.001$), TRPC6 ($p<0.001$), and p22pHox ($p<0.01$) in IS-induced IC21 macrophages (Figure 6a-c).

However, pretreatment with effective concentrations of CDB nanoformulation dose dependently decreased the stress markers in IS-induced IC21 macrophages. Alongside, the increased NO release triggered by the inflammatory stimulus was also ameliorated by CBD nanoformulation (Figure 6d).

Additionally, the intracellular ROS mediated by IS with or without CBD was determined using DCFDA molecular probes on a flow cytometer. As seen in the Figure 6e, we observed a peak shift towards the right in IS-stimulated macrophages, indicating a higher accumulation of intracellular ROS. In contrast, the macrophages that were exposed to CBD nanoformulation showed a leftward peak shift that is comparable to the control, which denoted a reduction in ROS levels.

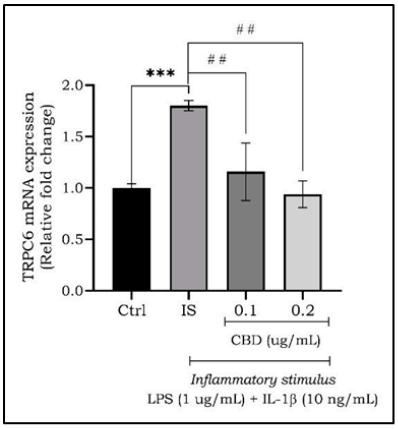

(a)

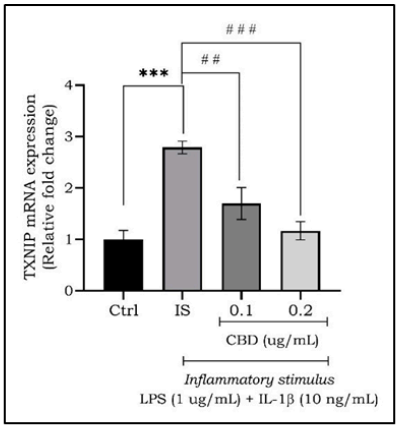

(b)

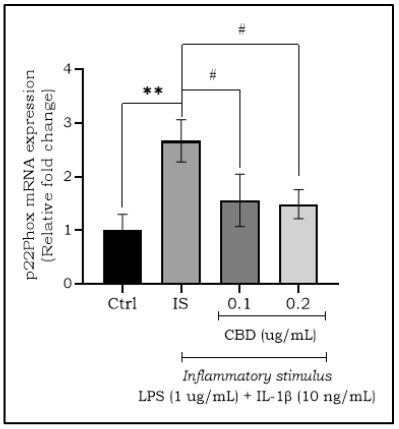

(c)

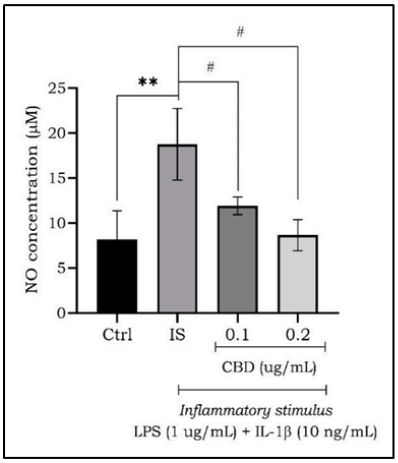

(d)

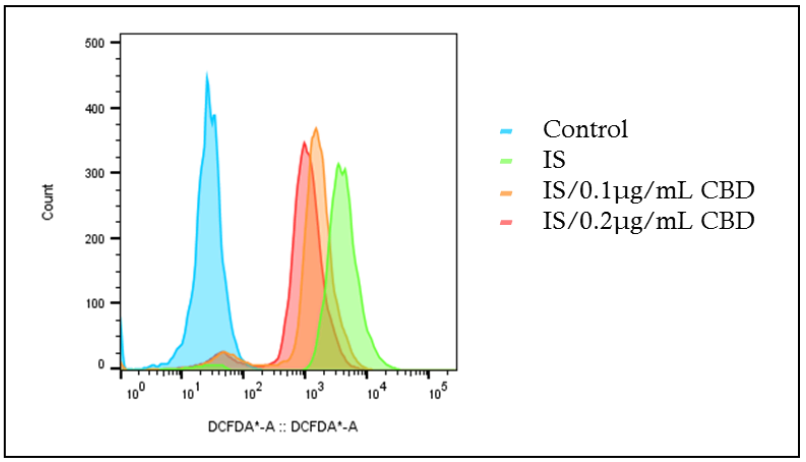

(e)

Figure 6: Effect of CBD nanoformulation on the mRNA expression of oxidative stress markers such as TRPC6 (a), TXNIP (b), p22PHox (c), and NO production assessment using Griess assay (d) in IC21 macrophages exposed to IS. Determination of intracellular ROS in IC21 macrophages under IS (e). Data in the bar graph are represented as mean ± S.D. *p<0.05, **p<0.01, ***p<0.001. *compared to control; #compared to IS. IS in the figure represents inflammatory stimulus.

4. Discussion

Osteoarthritis (OA) is a degenerative joint disease that is characterized by cartilage degradation, synovial inflammation, and pain [23]. Although symptomatic pain relief remains the primary and major goal to treating OA, pharmacological interventions to date lack to cure for the course of the illness. Alternative approaches to strategically preserve cartilage and lower inflammation at a molecular level while alleviating pain are in urgent need. In this line, CBD has recently gained significant attention for its anti-inflammatory, analgesic properties, which are key regulatory pathways in the treatment of OA. Because of its natural properties, CBD offers a promising therapeutic option while favouring safety, unlike anti-inflammatory steroids and NSAIDs that are currently prescribed.

While a handful of studies have evaluated the anti-inflammatory effects of CBD, most of them have utilized the extracts prepared using conventional formulations. This, on the other hand, limits the bioavailability of CBD by posing rapid metabolism in the system and impairs a prolonged rescue effect on the inflammatory parameters. To address this concern, recent advances in the field of nano-medicine and nanotechnology-based drug delivery systems have shown that nano-formulations of drugs, including CBD, can significantly enhance their pharmacokinetic and therapeutic profiles. For instance, Taha et al. demonstrated that CBD formulated as nanostructured lipid carriers significantly enhanced its oral bioavailability in rats, highlighting the potential of nano-based delivery systems for improving CBD's pharmacokinetic profile [24]. Despite these advances, there remains a limited number of

preclinical studies evaluating the therapeutic efficacy of such nano-formulated CBD, especially industrial grade formulations, in a relevant disease model. Building upon these findings, our study explores the impact of a proprietary CBD nanoformulation in an MIA-induced osteoarthritis model in SD rats.

A previous sub-chronic study has identified the No Observed Adverse Effect Level (NOAEL) of oral CBD at approximately 150 mg/kg/day over 14 days and 140 mg/kg/day over 90 days using a pure hemp-derived CBD isolate [20]. With this literature, our study employed to use 200 mg/kg as the highest dose, which was strategically decided to evaluate the safety profile beyond the established NOAELs. We demonstrated no significant toxicity in rats that were orally administered with our CBD nanoformulation up to 200 mg/kg, with all vital organs being normal observed through biochemical parameters and histological analyses. Henceforth, we decided to use 200 mg/kg as the highest dosage, and half of the high dose, i.e., 100 mg/kg, as the lowest dose to evaluate the efficacy of CBD nanoformulation in OA-induced rats.

MIA disturbs the cellular metabolism and causes chondrocyte death, which leads to cartilage damage and inflammation. This is a well-established chemical-mediated model for OA that closely mimics human joint inflammation and cartilage breakdown [5, 25]. In contrast to the commonly used 1–1.5 mg/knee MIA dosage for inducing OA in rats, we employed a higher dose of 3 mg/knee. This dosage was selected to establish a more aggressive model of joint inflammation and degeneration, better mirroring the chronic pathological features observed in human OA. Previous studies have shown that higher MIA doses induce more extensive cartilage degradation, synovial inflammation, and pain behaviours in a dose-dependent manner [26, 27], hence making a robust model to evaluate the effectiveness of the CBD nanoformulation under conditions that closely simulate severe OA.

OA rats exhibited impaired gait, evidenced by a reduced stride length, which is commonly associated with joint pain and stiffness. Radiographic evaluations provided evidence of deformity of knee joints in OA rats. CBD treatment effectively improved joint function and structure. The stride length was restored, and the knee joint space was improved in OA rats treated with CBD nanoformulation. Histological analyses of knee sections further confirmed the protective effects of CBD against cartilage degradation. Untreated OA rats showed complete loss of articular cartilage, whereas high-dose CBD treatment partially preserved cartilage integrity and joint architecture. The retention of Safranin-O staining in CBD-treated knees indicates greater preservation of glycosaminoglycans and proteoglycans, critical components of cartilage extracellular matrix, thereby suggesting a chondroprotective effect.

Furthermore, the anti-inflammatory potential of CBD was evident from the reduced infiltration of inflammatory cells in joint sections of high-dose treated animals. Chronic inflammation plays a central role in OA pathogenesis, driving cartilage breakdown and matrix remodelling through cytokine release. The attenuation of excessive recruitment of inflammatory cells by CBD limits the progression of inflammation-induced cartilage degradation in OA rats. Furthermore, as macrophages are the key players of inflammation, we studied the action of CBD on macrophages in vitro. The macrophages were induced with LPS and IL-1β b to simulate an inflammatory microenvironment. This stimulation increased the oxidative stress, inflammation, thereby increasing nitric oxide synthesis. All these were subsided upon treatment with CBD nanoformulations.

Collectively, the dose-dependent therapeutic efficacy observed in this study suggests that CBD shows a pronounced anti-osteoarthritic effect in terms of cartilage preservation, joint function restoration, and inflammation reduction, underscoring the promise of CBD-based interventions in OA management.

5. Conclusion

The present study underscores the therapeutic potential of a novel CBD nanoformulation in the treatment of osteoarthritis. By effectively modulating the joint deformities, reducing the pro-inflammatory cytokines, and exhibiting protection to cartilage architecture, the formulation addresses key pathological features of OA in rats. The enhanced efficacy observed in this model may be due to its improved bioavailability and tissue penetration capability achieved by the nanoformulation. Future studies will focus on pharmacokinetics, long-term safety, and clinical validation in human OA patients.

Declarations

Author contribution: Ravichandran Jayasuriya: Conceptualization, Data curation, Formal analysis, Methodology, Software, Writing – original draft. Rajappan Chandra Sathish Kumar: Conceptualization, Project administration, Resources, Investigation, Validation, Supervision, Funding acquisition. Kunka Mohanram Ramkumar: Conceptualization, Project administration, Resources, Investigation, Validation, Visualization, Writing – review; editing, Supervision, Funding acquisition. All authors agree to be accountable for all aspects of work ensuring integrity and accuracy. All authors read and approved the final manuscript.

Funding: This study was supported by Unique Therapeutics Global, Czech Republic, which provided the proprietary CBD nanoformulation used in the experiments.

Declaration of competing interests: The authors declare no conflict of interest beyond procurement of CBD nanoformulation and funding from Unique Therapeutics Global, Czech Republic.

References

[1] M. Langworthy, V. Dasa, A.I. Spitzer, Knee osteoarthritis: disease burden, available treatments, and emerging options, Therapeutic Advances in Musculoskeletal Disease 16 (2024).

[2] E. Sanchez-Lopez, R. Coras, A. Torres, N.E. Lane, M. Guma, Synovial inflammation in osteoarthritis progression, Nature Reviews Rheumatology 18(5) (2022) 258-275.

[3] Y. He, Z. Li, P.G. Alexander, B.D. Ocasio-Nieves, L. Yocum, H. Lin, R.S. Tuan, Pathogenesis of Osteoarthritis: Risk Factors, Regulatory Pathways in Chondrocytes, and Experimental Models, Biology 9(8) (2020) 194.

[4] H. Akkiraju, A. Nohe, Role of Chondrocytes in Cartilage Formation, Progression of Osteoarthritis and Cartilage Regeneration, Journal of Developmental Biology 3(4) (2015) 177-192.

[5] L. Zheng, Z. Zhang, P. Sheng, A. Mobasheri, The role of metabolism in chondrocyte dysfunction and the progression of osteoarthritis, Ageing Research Reviews 66 (2021) 101249.

[6] I. Ghlichloo, V. Gerriets, Nonsteroidal Anti-Inflammatory Drugs (NSAIDs), StatPearls, Treasure Island (FL) ineligible companies. Disclosure: Valerie Gerriets declares no relevant financial relationships with ineligible companies., 2025.

[7] A. Al-Saeed, Gastrointestinal and Cardiovascular Risk of NonsteroidalAnti-inflammatory Drugs, Oman Medical Journal 26(6) (2011) 385-391.

[8] M. Phillips, H. Curtis, B. Portmann, N. Donaldson, A. Bomford, J. O'Grady, Antioxidants versus corticosteroids in the treatment of severe alcoholic hepatitis—A randomised clinical trial, Journal of Hepatology 44(4) (2006) 784-790.

[9] M. Bryk, K. Starowicz, Cannabinoid-based therapy as a future for joint degeneration. Focus on the role of CB(2) receptor in the arthritis progression and pain: an updated review, Pharmacological reports : PR 73(3) (2021) 681-699.

[10] M.Y. Ansari, N. Ahmad, T.M. Haqqi, Oxidative stress and inflammation in osteoarthritis pathogenesis: Role of polyphenols, Biomedicine & pharmacotherapy = Biomedecine & pharmacotherapie 129 (2020) 110452.

[11] J. Fernández-Ruiz, O. Sagredo, M.R. Pazos, C. García, R. Pertwee, R. Mechoulam, J. Martínez-Orgado, Cannabidiol for neurodegenerative disorders: important new clinical applications for this phytocannabinoid?, British Journal of Clinical Pharmacology 75(2) (2013) 323-333.

[12] H.T. Philpott, M. O'Brien, J.J. McDougall, Attenuation of early phase inflammation by cannabidiol prevents pain and nerve damage in rat osteoarthritis, Pain 158(12) (2017) 2442-2451.

[13] N. Soliman, S. Haroutounian, A.G. Hohmann, E. Krane, J. Liao, M. Macleod, D. Segelcke, C. Sena, J. Thomas, J. Vollert, K. Wever, H. Alaverdyan, A. Barakat, T. Barthlow, A.L.H. Bozer, A. Davidson, M. Diaz-delCastillo, A. Dolgorukova, M.I. Ferdousi, C. Healy, S. Hong, M. Hopkins, A. James, H.B. Leake, N.M. Malewicz, M. Mansfield, A.K. Mardon, D. Mattimoe, D.P. McLoone, G. Noes-Holt, E.M. Pogatzki-Zahn, E. Power, B. Pradier, E. Romanos-Sirakis, A. Segelcke, R. Vinagre, J.A. Yanes, J. Zhang, X.Y. Zhang, D.P. Finn, A.S.C. Rice, Systematic review and meta-analysis of cannabinoids, cannabis-based medicines, and endocannabinoid system modulators tested for antinociceptive effects in animal models of injury-related or pathological persistent pain, Pain 162(1) (2021) S26-S44.

[14] S.L. Dunn, J.M. Wilkinson, A. Crawford, C.L. Le Maitre, R.A.D. Bunning, Cannabinoid WIN-55,212-2 mesylate inhibits interleukin-1β induced matrix metalloproteinase and tissue inhibitor of matrix metalloproteinase expression in human chondrocytes, Osteoarthritis and Cartilage 22(1) (2014) 133-144.

[15] U. Anand, B. Jones, Y. Korchev, S.R. Bloom, B. Pacchetti, P. Anand, M.H. Sodergren, CBD Effects on TRPV1 Signaling Pathways in Cultured DRG Neurons, Journal of Pain Research Volume 13 (2020) 2269-2278.

[16] G.K. Silva-Cardoso, W. Lazarini-Lopes, J.E. Hallak, J.A. Crippa, A.W. Zuardi, N. Garcia-Cairasco, C.R.A. Leite-Panissi, Cannabidiol effectively reverses mechanical and thermal allodynia, hyperalgesia, and anxious behaviors in a neuropathic pain model: Possible role of CB1 and TRPV1 receptors, Neuropharmacology 197 (2021) 108712.

[17] S. Atalay, I. Jarocka-Karpowicz, E. Skrzydlewska, Antioxidative and Anti-Inflammatory Properties of Cannabidiol, Antioxidants 9(1) (2019) 21.

[18] D. Jantas, M. Leśkiewicz, M. Regulska, M. Procner, P. Warszyński, W. Lasoń, Protective Effects of Cannabidiol (CBD) against Qxidative Stress, but Not Excitotoxic-Related Neuronal Cell Damage—An In Vitro Study, Biomolecules 14(5) (2024) 564.

[19] G. Calabrese, A. Zappalà, A. Dolcimascolo, R. Acquaviva, R. Parenti, G.A. Malfa, Phytochemical Analysis and Anti-Inflammatory and Anti-Osteoarthritic Bioactive Potential of Verbascum thapsus L. (Scrophulariaceae) Leaf Extract Evaluated in Two In Vitro Models of Inflammation and Osteoarthritis, Molecules 26(17) (2021) 5392.

[20] R.G. Henderson, T.W. Lefever, M.M. Heintz, K.R. Trexler, S.J. Borghoff, M.O. Bonn-Miller, Oral toxicity evaluation of cannabidiol, Food and Chemical Toxicology 176 (2023) 113778.

[21] M. Bryk, J. Chwastek, J. Mlost, M. Kostrzewa, K. Starowicz, Sodium Monoiodoacetate Dose-Dependent Changes in Matrix Metalloproteinases and Inflammatory Components as Prognostic Factors for the Progression of Osteoarthritis, Frontiers in Pharmacology 12 (2021).

[22] S.-B. Kwon, G. Chinta, S. Kundimi, S. Kim, Y.-D. Cho, S.-K. Kim, J.-Y. Ju, K. Sengupta, A Blend of Tamarindus Indica and Curcuma Longa Extracts Alleviates

Monosodium Iodoacetate (MIA)-Induced Osteoarthritic Pain and Joint Inflammation in Rats, Journal of the American Nutrition Association 43(1) (2023) 48-58.

[23] R. Sen, J.A. Hurley, Osteoarthritis, StatPearls, Treasure Island (FL) ineligible companies. Disclosure: John Hurley declares no relevant financial relationships with ineligible companies., 2025.

[24] I.E. Taha, M.A. ElSohly, M.M. Radwan, R.M. Elkanayati, A. Wanas, P.H. Joshi, E.A. Ashour, Enhancement of cannabidiol oral bioavailability through the development of nanostructured lipid carriers: In vitro and in vivo evaluation studies, Drug Delivery and Translational Research (2024).

[25] Z. Bao, M. Chen, C. Li, Q. Shan, Y. Wang, W. Yang, Monosodium iodoacetate-induced subchondral bone microstructure and inflammatory changes in an animal model of osteoarthritis, Open Life Sciences 17(1) (2022) 781-793.

[26] R. Combe, S. Bramwell, M.J. Field, The monosodium iodoacetate model of osteoarthritis: a model of chronic nociceptive pain in rats?, Neuroscience Letters 370(2-3) (2004) 236-240.

[27] C. Guingamp, P. Gegout-Pottie, L. Philippe, B. Terlain, P. Netter, P. Gillet, Mono-iodoacetate-induced experimental osteoarthritis. A dose-response study of loss of mobility, morphology, and biochemistry, Arthritis & Rheumatism 40(9) (2005) 1670-1679.